Dynamical phase diagram of the van Hemmen model of spin glass

1994 J. Phys. A: Math. Gen. 27 671

(http://iopscience.iop.org/0305-4470/27/3/013)

J. Phys. A: Math. Gen. 27 (1994) 671–681. Printed in the UK

Dynamical phase diagram of the van Hemmen model of spin glass

Francisco A Tamarit and Evaldo M Fleury Curado

Centro Brasileiro de Pesquisas Físicas/CNPq Rua Xavier Sigaud 150, 22290, Rio de Janeiro, Brazil

Received 28 July 1993

Abstract. The dynamical behaviour of the van Hemmen model of spin glass is studied by comparing the time evolution of two configurations subjected to the same thermal noise. It was found that the system undergoes several dynamical phase transitions among the paramagnetic, ferromagnetic, spin-glass and mixed phases. The dynamical phase diagram seems to be in good agreement with the static one. In the spin glass phase, the system presents a quite different dynamical behaviour from that found in short-range spin glass models as well as in the Sherrington–Kirkpatrick model.

1. Introduction

The spreading of damage concept, originally introduced to study the structure of the phase space in complex systems (cellular automata, non-symmetric neural nets and spin glasses, etc.) has also been shown to be an important tool in the study of magnetic systems [1–11]. In the last few years, this technique has been applied to a great variety of models in order to understand the possible connections between their dynamical and thermodynamical properties and to obtain information on the structure of the phase space of unsolved models like short-range spin glasses, among others [8–12].

The method is based on the time evolution comparison of two or more configurations submitted to the same thermal noise. By analysing the behaviour of the Hamming distance as a function of the temperature and the initial conditions, a *dynamical phase diagram* of the system may be constructed.

Monte Carlo simulations on diverse spin models suggest a strong correlation between the static and dynamical phases of magnetic systems. Nevertheless, due to the lack of a general theory for the spreading of damage method, it is not possible to guarantee that they will necessarily agree. Indeed, for some models, the existence of relationships between static and dynamical quantities has been analytically proved [13–16]. Nevertheless, this technique always allows one to obtain information on the free energy landscape of the model by studying the dependence of the Hamming distance evolution on the initial conditions.

The spin glass theory has been a difficult problem in statistical mechanics (see for example [19]). For many years there has been great controversy on whether the spin glass transition is either of thermodynamical or of dynamical nature. However, simulations [20] and phenomenological scaling arguments at zero temperature [21] suggested the existence of a true thermodynamical phase transition. Until now, only

0305-4470/94/030671+11 $07.50

mean field models are exactly tractable, but, they require sophisticated mathematical tools [17, 18]. In the last few years spin glasses have been studied also through the spreading of damage method. When submitted to heat bath dynamics the three-dimensional spin glass has three regimes: at high temperature the Hamming distance vanishes; at intermediate temperatures the Hamming distance is non-zero and it is independent of the initial distance; at low temperatures the Hamming distance depends on the initial conditions. For the Sherrington–Kirkpatrick (SK) model, Derrida found only two regimes, both with non-zero Hamming distance. In the low temperature regime its value depends on the initial distance but at high temperatures it does not.

In this paper we study the spreading of damage on the spin glass mean field model introduced by van Hemmen [17]. It is the simplest model that contains both randomness and frustration. It is exactly soluble, and, unlike the Sherrington–Kirkpatrick [18] model, its solution does not require the use of the replica trick. In spite of being non-realistic, mean field models give a first qualitative understanding of the thermodynamical behaviour. It is then interesting to study the similarities and differences among the dynamical behaviour of the van Hemmen model, the SK model and the short-range models, as well as whether the dynamical phase diagram coincides with the static one.

The present paper is organized as follows: In section 2 we introduce the van Hemmen model and describe the thermodynamical phase diagram obtained in [17]. In section 3 the method used for the study of the time evolution of the Hamming distance is presented. In section 4 we analyse the dynamical phase diagram and compare it with the static one. Finally, in section 5 the main results are discussed.

2. Model

The van Hemmen model of spin glass consists of a fully connected net of N Ising spins described by the following Hamiltonian [17]:

$$H=-\frac{J_0}{N}\sum_{(i,j)}^{N} S_iS_j-\sum_{(i,j)}^{N} J_{ij}S_iS_j-h\sum_{i}^{N} S_i \tag{1}$$

where (i,j) denotes a sum over all possible pairs of spins, J_0 represents a ferromagnetic coupling, h is an external magnetic field, and the J_{ij}s are the spin glass random couplings given by

$$J_{ij}=\frac{J}{N}(\xi_i\eta_j+\xi_j\eta_i). \tag{2}$$

The ξ_is and the η_is ($i=1,\ldots,N$) are independent, identically distributed random variables with zero mean value. In particular, we restrict ourselves to the case in which they can take the values $+1$ and -1.

Let us briefly describe the thermodynamical phase diagram of the model.

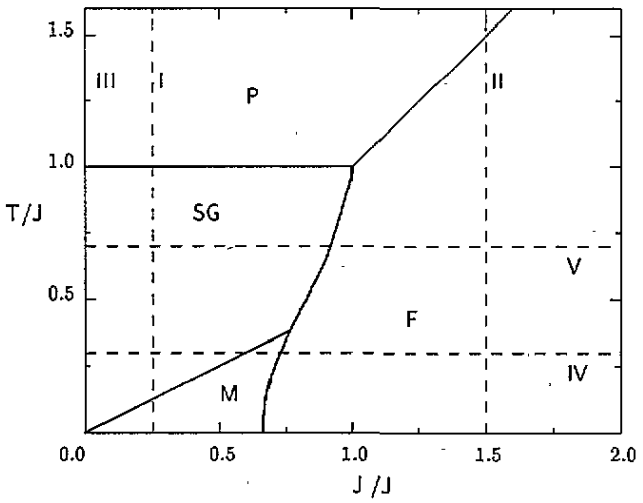

Figure 1. The phase diagram of the van Hemmen model obtained in [17] and the cuts I, II, III, IV and V (cut III is along the $J_0/J=0$ axis).

Following van Hemmen [17] we define three order parameters, namely

$$m=\lim_{N\to\infty}\frac{1}{N}\sum_{i=1}^{N}S_i \tag{3}$$

$$q_1=\lim_{N\to\infty}\frac{1}{N}\sum_{i=1}^{N}\xi_i S_i \tag{4}$$

$$q_2=\lim_{N\to\infty}\frac{1}{N}\sum_{i=1}^{N}\eta_i S_i. \tag{5}$$

In the limit $N\to\infty$ the free energy is given by

$$f(\beta)=\min\left(\frac{1}{2}m^2+Jq_1q_2-\frac{1}{\beta}\langle\ln\cosh(\beta(J_0m+J(q_2\xi+q_1\eta)+hm))\rangle\right) \tag{6}$$

where min indicates that the argument has to be evaluated at the values of m, q_1 and q_2 that minimize it and $\langle\ldots\rangle$ denotes an average over the ξs and the ηs. It can be shown that these minimum corresponds always to the case $q_{1N}=q_{2N}=q$, and then the mean field equations take the form

$$\begin{aligned} m&=\langle\tanh(\beta(J_0m+q(\xi+\eta)+h))\rangle\\ q&=\tfrac{1}{2}\langle(\xi+\eta)\tanh(\beta(J_0m+q(\xi+\eta)+h))\rangle. \end{aligned} \tag{7}$$

The phase diagram at zero magnetic field obtained by van Hemmen is shown in figure 1. The paramagnetic phase corresponds to the trivial solution $m=q=0$. When $m\neq0$ and $q=0$ the system is ferromagnetic and when $q\neq0$ and $m=0$ the system is a spin glass. It also presents a *mixed* phase for which both q and m are non-zero.

3. Method

We study the behaviour of the system described by (1) with zero magnetic field ($h=0$) when ruled by a heat bath Monte Carlo dynamics. At any time t, a site is chosen randomly and its spin is updated by setting the new value of S_i at time $t+\mathrm{d}t$ according to the following rule:

$$s_i(t+\mathrm{d}t)=\begin{cases}+1 & \text{with probability } [1+\mathrm{e}_i^{-2\beta h_i}]^{-1}\\ -1 & \text{with probability } [1+\mathrm{e}_i^{2\beta h_i}]^{-1}\end{cases} \tag{8}$$

where h_i is the local field at site i defined as

$$h_i=\sum_{j\neq i}^{N} J_{ij}S_j. \tag{9}$$

Since the updating is done sequentially, the natural scale for the Monte Carlo step is $1/N$.

The spreading of damage method consists of the following procedure: we take an equilibrium configuration of the system $\{S_i(0)\}$ at a given temperature and make a copy of it. This copy is damaged by inverting a certain fraction of its spins. Let us call this damaged copy $\{S_i'(0)\}$. Next we let both configurations evolve according to (8) and with the same random sequence, and calculate the time averaged Hamming distance Δ, with $\Delta(t)$ given by

$$\Delta(t)=\frac{1}{2N}\sum_{i=1}^{N}(S_i(t)-S_i'(t))^2. \tag{10}$$

This time average is always calculated over $r=500$ Monte Carlo steps. For each temperature, $\langle\Delta\rangle$ is obtained by averaging over a set of M samples with different initial conditions, random sequence and spin glass couplings. M depends both, on the size of the system and on the temperature. These procedure is then repeated for different values of the ferromagnetic coupling J_0 and temperature.

Note that $\Delta(t)$ measures the fraction of sites for which the two configurations are different at a given time t. If at any time they meet, that is, they become identical, they will remain identical for all the subsequent steps. Let us define $\langle dh\rangle$ as the mean Hamming distance averaged only over the surviving samples, i.e. over those samples whose Hamming distance does not become zero up to time τ. The $\langle dh\rangle$ and $\langle\Delta\rangle$ are related through the following equation:

$$\langle\Delta\rangle=P(\tau)\langle dh\rangle \tag{11}$$

where $P(t)$ is the fraction of samples that have survived up to time t. When working on a finite lattice, $P(t)$ is expected to depend both on the size of the system N and on the time cut-off τ, while $\langle dh\rangle$ seems to be rather constant. Then, in what follows, we calculate the $\langle dh\rangle$ and $P(\tau)$ instead of $\langle\Delta\rangle$.

In order to study the dependence of $\langle dh\rangle$ on the initial damage, we consider only two different kind of initial conditions:

random: spins are inverted with probability $\frac{1}{2}$;
opposite: each spin is inverted.

Since the lattice is fully connected, we are limited to working with small systems. For

any point of the diagram the calculations were always performed for $N=128$, $N=256$ and $N=512$.

4. Dynamical phase diagram

Due to the full connectivity of the model, a complete calculation of the dynamical phase diagram would require a huge numerical effort. Then, we restrict ourselves to analysing the behaviour of the system along the five cuts in the (T/J, J_0/J) phase displayed in figure 1. Three cuts correspond to fixed J_0/J($J_0/J=0.25$, 1.5 and 0) and the other two to fixed T/J($T/J=0.3$ and 0.7). The J value was fixed to be 1, and henceforth we will refer to the J_0/J and T/J axes as J_0 and T, respectively.

In figure 2(a) we present the results for $J_0=0.25$ (cut I). The system displays three different dynamical regimes:

- for low temperatures ($T<T_1\approx 0.11$), $\langle dh\rangle \neq 0$ and its value depends on the initial damage between the configurations;
- in the intermediate regime ($T<T_1<T_2\approx 0.975$), $\langle dh\rangle \neq 0$ and its value is independent of the initial damage;
- for high temperatures ($T>T_2$) $\langle dh\rangle$ is always zero.

The lower transition temperature $T_1\approx 0.11$ is in good agreement with the mixed-spin glass transition temperature calculated from (7), and it does not seem to depend on the size of the system as far as we can infer from our simulations. On the other hand, it is more difficult to determine T_2 because, close to this transition, the surviving probability $P(\tau)$ goes abruptally to zero (see figure 2(b)) and depends strongly on the size of the system and on the time cut-off τ. The computational time needed to get an adequate number of surviving samples increases in such a way that makes impossible to obtain a more accurate value for T_2. However, although its value is lower than the corresponding thermodynamical transition temperature $T_c=1$, it seems to approach this values as N increases. We note that, unlike other mean-field models (for example the ferromagnetic Ising model or Sherrington–Kirkpatrick model), in this case $\langle dh\rangle$ falls abruptly near the spin glass–paramagnetic temperature transition. But as N increases, this jump seems to decrease. It is impossible to infer from our simulations whether this discontinuous behaviour exists in the thermodynamical limit or is due to finite-size effects.

In figure 2(c) we show the behaviour of $\langle t\rangle$ as a function of T, where $\langle t\rangle$ is defined as the averaged time needed by two configurations with random initial conditions to meet in the phase space. Unlike $\langle dh\rangle$, it is easy to calculate $\langle t\rangle$ near T_2 because, in this region almost no pair of configurations survives. As N increases $\langle t\rangle$ seems to diverge at two different temperatures. Here again, the lower one does not depend in a sensible way on the size of the system while the higher one increases as N increases. Nevertheless, the cusp form of the curve leads us to believe that the system actually undergoes a dynamical transition at a temperature close to the spin glass–paramagnetic transition temperature.

In order to obtain more information about the free energy landscape of the system in the low and intermediate phases, in figure 3 we present the distribution of the Hamming distance for those pairs of configurations with random initial conditions that have survived at $t=\tau=500$ *MCS*, for $J_0=0.25$, $N=265$, an for both $T=0.075$ (below T_1, figure 3(a)) and $T=0.20$ (above T_1 figure 3(b)). At $T=0.2$, in the intermediate

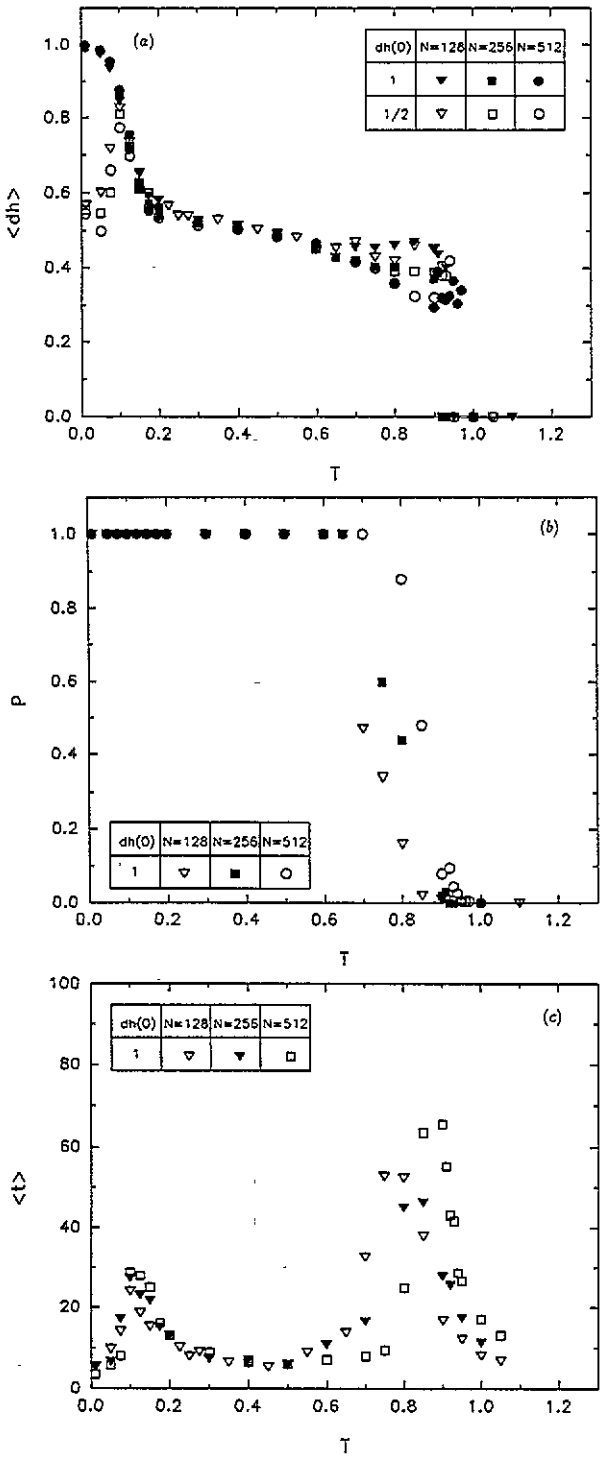

Figure 2. Damage for $J_0/J = 0.25$ as a function of the temperature: (*a*) distance $\langle dh \rangle$ between two configurations provided they are still different; (*b*) the fraction $P(t)$ of non-identical configurations; and (*c*) the time $\langle t \rangle$ needed for two configurations to become identical.

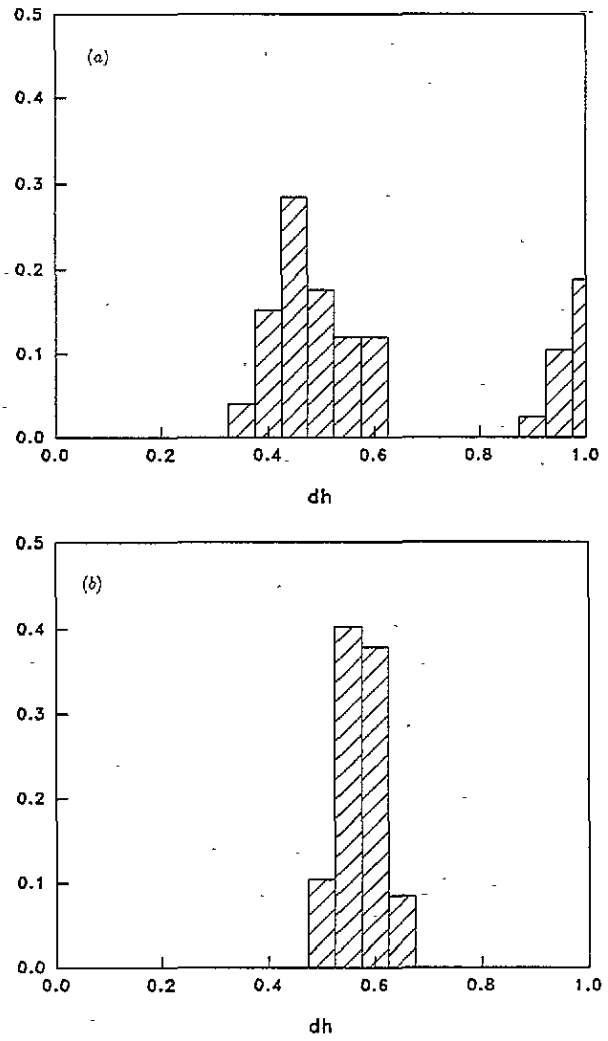

Figure 3. The distribution of distances for $J_0/J=0.25$ and $N=256$: (*a*) for $T=0.075$ (mixed phase); and (*b*) for $T/J=0.2$ (spin glass phase).

spin glass phase, the system presents only one attractor, being the histogram sharply peaked around $\langle dh\rangle \approx \frac{1}{2}$. In terms of the free energy landscape, we can conclude that, if the system has a multivalley structure, all these valleys should be equally spaced. The $T=0.075$ histogram displays a double peaked distribution around $\langle dh\rangle = 0.5$ and $\langle dh\rangle = 1.0$. In particular, note that the peak around $\langle dh\rangle = 0.5$ is wider than the peak found at $T=0.2$, showing that the system has a multivalley structure with different Hamming distance among the valleys.

We have performed the same calculations for the cut $J_0=0.5$ and the results are qualitatively similar, displaying the three dynamical phases found for cut I. Here again, the lower critical temperatures $T_1 \approx 0.23$ is in a good agreement with the corresponding thermodynamical critical temperature and T_2 depends on the size of the system, but as N increases, it seems to approach the static critical temperature $T_c=1$, corresponding to the spin glass–paramagnetic transition.

In figure 4 we show the behaviour of $\langle dh \rangle$ versus T for $J_0 = 1.5$. Here, the system displays the typical mean-field Ising ferromagnetic behaviour, with only two regimes: the low temperature one, where $\langle dh \rangle \neq 0$ and its value is independent of the initial damage between the configurations, and a high temperature one where $\langle dh \rangle$ always vanishes. The dynamical transition temperature is lower than the thermodynamical transition temperature $T_c = 1.5$, and it depends on the size of the system N, approaching this value as N increases.

Figure 5 presents the $J_0 = 0$ behaviour of $\langle dh \rangle$. It is interesting to note that, in total agreement with the thermodynamical phase diagram, the mixed phase does not appear at finite temperature. The system presents only two regimes: the intermediate and the high temperature ones of figure 2(*a*). This is a surprising result: even starting with opposite configurations, for any finite value of T they will end up in two uncorrelated valleys. In this particular case the system can be decoupled into two non-interacting subsystems, each one with approximately half of the spin of the net. One subsystem is ferromagnetic and presents a low temperature dynamical phase in which the Hamming distance does not vanish. The other subsystem is anti-ferromagnetic, and due to the strong frustration it does not order, even at $T = 0$. Although this system is very similar to the Hopfield model for associative memory with only two stored patterns, they present a completely different dynamical behaviour. This difference is due to the fact that, unlike the van Hemmen model, the Hopfield model with two memories is not frustrated: it can also be decoupled into two non-interacting subsystem, but both of them are ferromagnetic.

Figures 6 and 7 show the $\langle dh \rangle$ versus J_0 behaviour of the system for $T = 0.3$ and $T = 0.7$. Note that close to the spin glass-ferro and to the spin glass-mixed static transitions the system undergoes a dynamical transition that can be determined with good accuracy. In figure 6 we observe that the system undergoes a second dynamical transition for higher values of the ferromagnetic coupling, but it does not agree with the transition value of the static diagram. We believe that this is due to the fact that this transition is a first-order one, and so is harder to determine numerically an accurate value of the corresponding parameter.

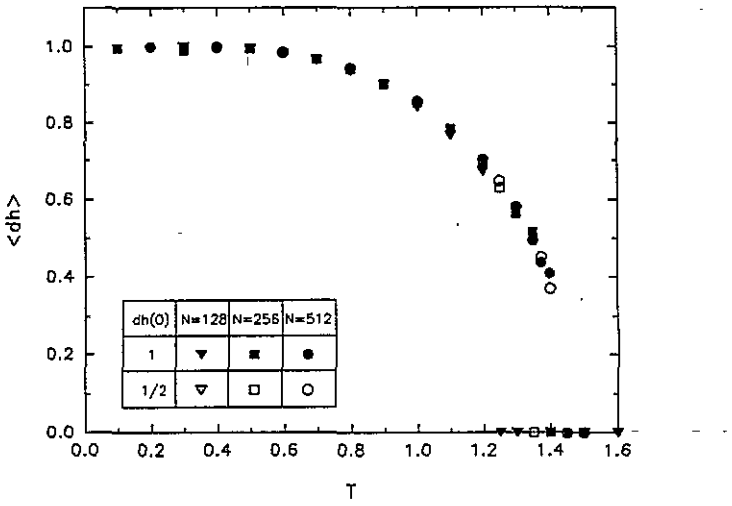

Figure 4. The distance $\langle dh \rangle$ for $J_0/J = 1.5$ as a function of the temperature.

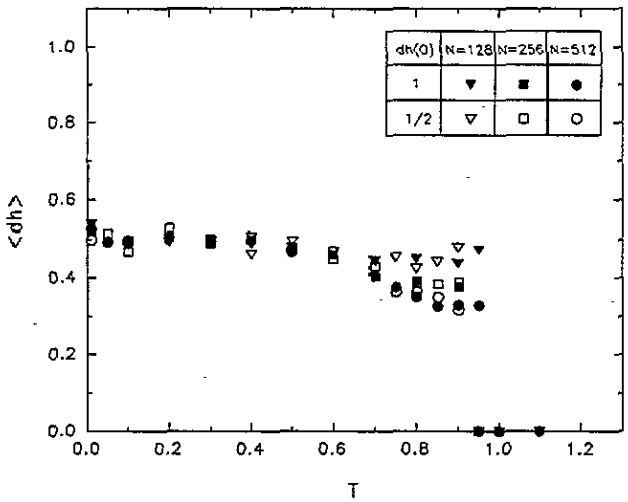

Figure 5. Distance $\langle dh \rangle$ between two configurations provided they are still different at $t = 500\ MCS$ versus T/J for $J_0/J = 0$.

5. Discussion

In this paper we have studied the Hamming distance behaviour of the van Hemmen model of spin glass, when submitted to a heat bath Monte Carlo process. The thermodynamical phase diagram obtained in [17] is compared with a dynamical one, based on the sensibility of the Hamming distance on the initial damage. The system undergoes different dynamical transitions which seem to be in good agreement with those static transitions found in [17]. Unfortunately, more accurate quantitive results are very difficult to obtain.

From the dynamical behaviour of the system presented in the former section, we observe that the strong correlation that exists between the statical and dynamical phase diagram can be summarized as follows:

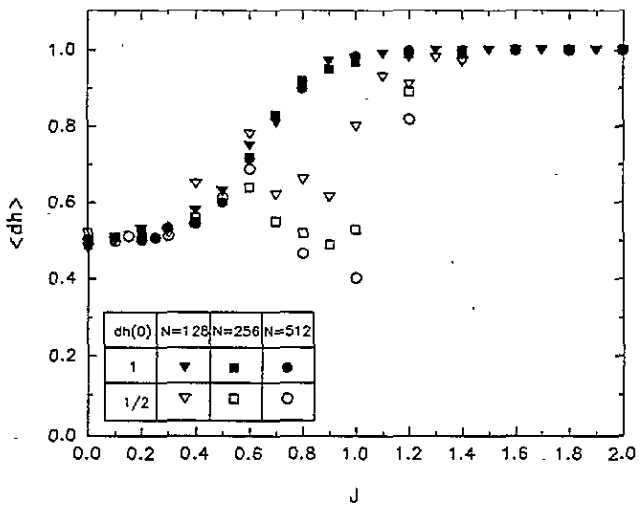

Figure 6. The distance $\langle dh \rangle$ for $T/J = 0.3$ as a function of J_0/J.

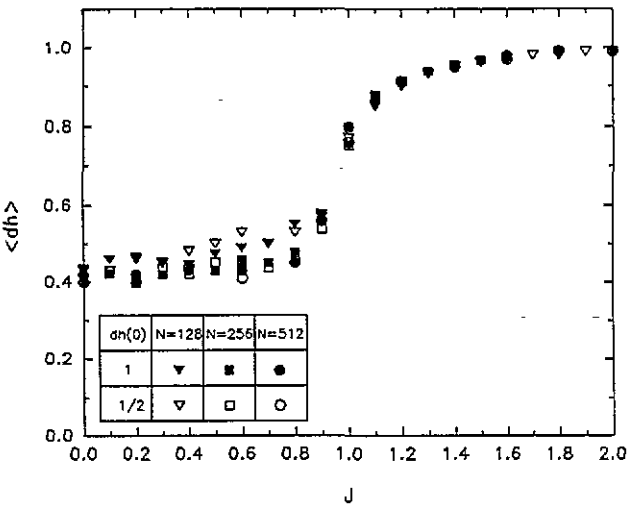

Figure 7. The distance $\langle dh \rangle$ for $T/J = 0.7$ as a function of J_0/J.

1. The *spin glass phase* of this model is characterized by a non-zero Hamming distance value that does not depend on the initial distance between the configurations and by a peaked distribution of distances. This behaviour is a novel result for a spin glass phase, since other systems studied (short-range model and the SK mean field model) display a spin glass phase characterized by a non-zero value of the Hamming distance which depends on the initial damage (as occurs in the mixed phase of the van Hemmen model).

2. In the *paramagnetic phase* the Hamming distance is always zero. This behaviour is also different from that found in other models: the SK mean field model in the paramagnetic phase presents a non-zero Hamming distance, and short-range models display an intermediate phase probably associated to a Griffiths phase in which the final distance is independent of initial distance.

3. In the ferromagnetic phase the Hamming distance is different from zero, and presents the usual behaviour found in ferromagnetic system at low temperatures.

4. In the mixed phase, the system presents the dynamical behaviour found in the spin glass phase for the SK model and for the 3D short-range Ising spin glass model.

It is not clear for us up to now why the van Hemmen model displays a completely different behaviour from that found in other spin glass model. In particular, the divergence between this model and the SK model in the spin glass and in the paramagnetic phase is surprising, since both models share the main properties, namely both have frustration, randomness and are fully connected. In fact, the only difference is due to the spin-glass coupling distribution.

Acknowledgments

The authors are deeply indebted to D Stariolo, A Coniglio, H Herrmann, L de Arcangelis and C Tsallis for useful discussions, and thank CNPq (Brazil) for financial support.

References

[1] Stanley H, Stauffer D, Kertés J and Hermann H 1987 *Phys. Rev. Lett.* **59** 2326
[2] Costa U M S 1987 *J. Phys. A: Math. Gen.* **20** L583
[3] Le Caer G 1989 *J. Phys. A: Math. Gen.* **22** L647
[4] Leroyer Y and Rouidi K 1991 *J. Phys. A: Math. Gen.* **24** 1931
[5] Barber M and Derrida B 1988 *J. Stat. Phys.* **51** 877
[6] Neumann A and Derrida B 1988 *J. Physique* **49** 1647
[7] Golinelli O and Derrida B 1988 *J. Physique* **49** 1663
[8] Derrida B and Weisbuch G 1987 *Europhys. Lett.* **4** 657
[9] da Cruz H, Costa U. and Curado E 1989 *J. Phys. A: Math. Gen.* **22** L651
[10] de Arcangelis L, Hermann H and Coniglio A 1990 *J. Phys. A: Math. Gen.* **21** L265
[11] Campbell I A and de Arcangelis L 1990 *Europhys. Lett.* **13** 587
[12] Nobre F D, Mariz A M and Souza E S 1992 *Phys. Rev. Lett.* **69** 13
[13] Coniglio A, de Arcangelis L, Herrmann H and Jan N 1989 *Europhys. Lett.* **8**, 315
[14] Mariz A 1990 *J. Phys. A: Math. Gen.* **26** 987
[15] Glotzer S C, Poole P H and Jan N 1992 *J. Stat. Phys.* **68** 895
[16] de Almeida R M C 1993 *J. Physique I* **3** 951
[17] van Hemmen J L 1982 *Phys. Rev. Lett.* **49** 409
[18] Sherrington D and Kirkpatrick S 1975 *Phys. Rev. Lett.* **35** 1792
[19] Binder K and Young A P 1986 *Rev. Mod. Phys.* **587** 801
[20] Bhatt R N and Young A P 1985 *Phys. Rev. Lett.* **54** 924
Ogielski A T and Morgenstein I 1985 *Phys. Rev. Lett.* **54** 928
[21] Bray A J and Moore M A 1984 *J. Phys. C: Solid State Phys.* **17** L463, L613
Bray A J 1988 *Comment Cond. Mat. Phys.* **14** 21